0026-895X/02/6201-22–29$7.00
MOLECULAR PHARMACOLOGY
Copyright © 2002 The American Society for Pharmacology and Experimental Therapeutics
Mol Pharmacol 62:22–29, 2002

Vol. 62, No. 1
1724/989973
Printed in U.S.A.

Inhibition of the Mitochondrial Permeability Transition by the Nonimmunosuppressive Cyclosporin Derivative NIM811

PETER C. WALDMEIER, JEAN-JACQUES FELDTRAUER, TING QIAN, and JOHN J. LEMASTERS

Nervous System Research, Novartis Pharma Ltd., Basel, Switzerland (P.C.W., J.-J.F.); and Department of Cell and Developmental Biology, University of North Carolina, Chapel Hill, North Carolina (T.Q., J.J.L.)

Received March 8, 2002; accepted March 21, 2002

This article is available online at http://molpharm.aspetjournals.org

ABSTRACT

Cyclosporin A (CsA) shows cytoprotective properties in many cellular and in vivo models that may depend on interference of the interaction of cyclophilin A with calcineurin or of cyclophilin D with the mitochondrial permeability transition (PT) pore. The nonimmunosuppressive cyclosporin derivative *N*-methyl-4-valine-cyclosporin (PKF220-384) inhibits the mitochondrial permeability transition (MPT) like CsA but without calcineurin inactivation. PKF220-384 has been used to discriminate between PT pore- and calcineurin mediated effects but is no longer available. Here, we evaluated the effects of another nonimmunosuppressive cyclosporin derivative, *N*-methyl-4-isoleucine-cyclosporin (NIM811) on the MPT. Using two newly developed microtiter plate assays, one measuring mitochondrial swelling from absorbance and the other measuring mitochondrial membrane potential from changes in safranin fluorescence, we show that NIM811 blocks the MPT induced by calcium and inorganic phosphate, alone or in combination with the dopaminergic neurotoxin 1-methyl-4-phenyl-1,2,3,6-tetrahydropyridine, the complex I inhibitor rotenone, and the prooxidant *t*-butylhydroperoxide. NIM811 was equipotent to CsA and half as potent as PKF220-384. Additionally, we show that NIM811 blocks cell killing and prevents in situ mitochondrial inner membrane permeabilization and depolarization during tumor necrosis factor-α–induced apoptosis to cultured rat hepatocytes. NIM811 inhibition of apoptosis was equipotent with CsA except at higher concentrations: CsA lost efficacy but NIM 811 did not. We conclude that NIM811 is a useful alternative to PKF220-384 to investigate the role of the mitochondrial permeability transition in apoptotic and necrotic cell death.

Permeabilization of mitochondrial membranes triggered by proapoptotic molecules and damage pathways is implicated as an important event in the control of cell death and survival and may be involved in both apoptosis and necrosis (for a recent review, see Kroemer and Reed, 2000). Inner membrane permeabilization causes dissipation of the mitochondrial membrane potential, uncoupling of oxidative phosphorylation, ATP depletion, and equilibration of small solutes and ions between the cytosol and the mitochondrial matrix. Solute influx into the matrix can cause swelling followed by rupture of the outer membrane and consequent efflux of proteins from the intermembrane space, including cytochrome *c*, procaspase 9, apoptosis-inducing factor, and endonuclease G. However, outer membrane permeabilization is not always related to inner membrane permeabilization but seems also to occur independently.

Several models of mitochondrial inner membrane permeabilization, specifically the mitochondrial permeability transition (MPT), are currently under discussion. Onset of the MPT is mediated by opening of a proteinaceous permeability transition (PT) pore that probably forms at contact sites between the inner and outer membranes. The PT pore is postulated to form through combination of the adenine nucleotide translocator of the inner membrane, the voltage dependent anion channel of the outer membrane, cyclophilin D (CypD) of the mitochondrial matrix and several other proteins, including the peripheral benzodiazepine receptor (outer membrane), creatine kinase (intermembrane space), hexokinase II (exterior side of the outer membrane), Bax and Bcl-2 (Zoratti and Szabò, 1995; Zamzami et al., 1998) An alternative model proposes that PT pores form by clustering of misfolded membrane proteins that are capped by chaperone-like regulatory and renaturing proteins such as CypD (He and Lemasters, 2002).

CypD binding to PT pores is required for the Ca^{2+}-dependent onset of the MPT. CypD also confers sensitivity of the MPT to cyclosporin A (CsA), and CsA is an effective and specific inhibitor of the MPT at submicromolar concentrations. However, CsA also binds cyclophilin A, leading to inhibition of calcineurin. Calcineurin dephosphorylates the ap-

ABBREVIATIONS: MPT, mitochondrial permeability transition; PT, permeability transition; CypD, cyclophilin D; CsA, cyclosporin A; PKF220-384, *N*-methyl-4-valine-cyclosporin; NIM811, *N*-methyl-4-isoleucine-cyclosporin; TNFα, tumor necrosis factor-α; FCCP, carbonyl cyanide *p*-(trifluoromethoxy)phenylhydrazone; MPP^+, 1-methyl-4-phenylpyridinium iodide; AM, acetoxymethyl ester; CsH, cyclosporin H; RB, respiratory buffer; HDM, hormonally defined medium; TMRM, tetramethylrhodamine methyl ester; NFκB, nuclear factor κB; *t*-BuOOH, *tert*-butylhydroperoxide.

optogenic protein Bad and enables it to bind other antiapoptotic Bcl-2 family members and trigger release of cytochrome *c* and other proapoptotic proteins from the intermembrane space (Kroemer and Reed, 2000). These two mechanisms, inhibition of the MPT and inhibition of calcineurin, may account for the many reports of cytoprotective actions of CsA against necrotic and apoptotic cell death (for example, see Nieminen et al., 1995; Matsuura et al., 1996; Halestrap et al., 1997; Bradham et al., 1998; Seaton et al., 1998; Scheff and Sullivan, 1999; Li et al., 2000). Attempts to distinguish between these two possibilities have been made in a few cases (Zamzami et al., 1996; Trost and Lemasters, 1997; Seaton et al., 1998) using the analog *N*-methyl-4-valine-cyclosporin (also called PKF220-384 or SDZ220-384), which is not immunosuppressive (Zenke et al., 1993) but binds to cyclophilins and inhibits the MPT (Petronilli et al., 1994). However, PKF220-384 is no longer available to researchers. Here, we provide evidence that another nonimmunosuppressive cyclosporin derivative, NIM811 (Rosenwirth et al., 1994), a compound that is still available, blocks the MPT induced by calcium plus phosphate in the presence and absence of enhancing agents, such as 1-methyl-4-phenylpyridinium and rotenone, in a fashion comparable with CsA and PKF220-384. NIM811 also blocked apoptotic cell death and mitochondrial depolarization and inner membrane permeabilization in situ in hepatocytes exposed to tumor necrosis factor-α (TNFα) in a fashion nearly identical to CsA but without the cytotoxicity of CsA at high concentrations.

Experimental Procedures

Materials

For photometric and fluorometric measurements, a Wallac Victor 1420 Multilabel Counter (PerkinElmer Wallac, Gaithersburg, MD) fitted with a 535DF35 filter or 485DF22 excitation/590DF35 emission filters, respectively (Omega Optical, Brattleboro, VT), was used.

Rotenone and carbonyl cyanide *p*-(trifluoromethoxy)phenylhydrazone (FCCP) were obtained from Sigma (Buchs, Switzerland), valinomycin and oligomycin from Sigma-Aldrich Chemie (Schnelldorf, Germany) and 1-methyl-4-phenylpyridinium iodide (MPP^+) from RBI (Natick, MA). Safranin T was purchased from Fluka (Buchs, Switzerland). TNFα was from R&D Systems, Inc. (Minneapolis, MN). Tetramethylrhodamine methylester and calcein AM were obtained from Molecular Probes (Eugene, OR). CsA, PKF220-384, NIM811, cyclosporin H (CsH; PKF037-839), and PSC833 are marketed by or are experimental compounds of Novartis.

Methods

Preparation of Mitochondria. Rat liver mitochondria were prepared by differential centrifugation essentially as described by Schnaitman and Greenawalt (1968). The liver of a rat weighing 300 to 400 g was washed three times with ice-cold isolation buffer (70 mM sucrose, 190 mM mannitol, 20 mM HEPES, 0.2 mM EDTA, brought to pH 7.5 with 1 M NaOH). The liver was cut into three to five pieces and then cross-chopped three times on a McIlwain tissue chopper (Mickle Laboratory Engineering Co., Gomshall, Surrey, UK). The chopped tissue was transferred into a 60-ml glass homogenizer fitted with a Teflon piston and further homogenized by two up-and-down strokes, diluted to 200 ml with ice-cold isolation buffer, and centrifuged at 650*g* for 10 min at 2°C. The supernatant, divided into eight ~25-ml portions, was recentrifuged at 7700*g* for 10 min at 2°C. The pellets were carefully suspended in 25 ml each of ice-cold washing buffer (same as isolation buffer, but without EDTA). The suspensions were recentrifuged at 7700*g* for 10 min at 2°C, the supernatants were discarded, and the pellets were suspended in 2 ml each of respiratory buffer (RB; 70 mM sucrose, 190 mM mannitol, 20 mM HEPES, 5 mM glutamate, and 0.5 mM malate, brought to pH 7.5 with 1 M NaOH). A total of about 20 ml of suspension was obtained, containing about 13 to 20 mg of mitochondrial protein/ml, as determined using a BCA assay (Pierce, Rockford IL). This suspension was stored on ice until further used.

Swelling Assay. Mitochondrial swelling caused by influx of solutes through open PT pores results in an increase in light transmission (i.e., a reduced turbidity; for discussion, see Zoratti and Szabò, 1995). This turbidity change offers a convenient and frequently used assay of the MPT by measurement of absorbance in mitochondrial suspensions. In the present study, the MPT induced by Ca^{2+} and inorganic phosphate (Ca^{2+}/P_i) was monitored by absorbance changes at 535 nm by adapting the procedure of Cassarino et al. (1999) to a microtiterplate assay.

Twenty microliters of the final mitochondrial suspension in RB as described above were pipetted into the wells of a Serocluster 96-well polystyrene microtiterplate (Costar, Cambridge MA), followed by 120 to 160 μl of RB (volume depending on what else was added). Cyclosporin derivatives were added in volumes of 20 μl of RB, and baseline values of all wells were measured subsequently. Five min after addition of the cyclosporins, 10 μl of $CaCl_2 \times 2H_2O$ (Ca^{2+}; final concentration 30 to 300 μM) dissolved in RB were added using a 12-tip pipetter to each row from A to H at 10-s intervals, followed 2 min later by 10 μl of $(NH_4)_2HPO_4$ (P_i; final concentration 1 mM) in RB, likewise at a 10-s interval per row. When additional compounds (MPP^+, rotenone) were used, they were added 2 min before Ca^{2+}, also at a 10-s interval per row.

Immediately after finishing pipetting, the plate was put into the reader (filter 535DF35, 535 nm), and the protocol for repetitive measurements was started with a timing such that the first well was measured exactly 2 min after pipetting P_i to the first row. Measurements were repeated every 2 min for a period of up to 28 min. All measurements were performed at room temperature. Data were expressed as means of the absorbance readings of quadruplicates ± S.E.M.

Measurement of Mitochondrial Membrane Potential. The same experimental conditions were used for the assessment of alterations of the mitochondrial membrane potential $\Delta\Psi$, except that safranin in 10 μl of RB was added after the cyclosporins at a final concentration of 15 μM. This concentration was determined beforehand as the optimal compromise between signal/baseline ratio and interference of safranin itself with swelling induced by Ca^{2+}/P_i (safranin tended to enhance Ca^{2+}/P_i-induced swelling at concentrations above 20 μM). Fluorescence readings were done using the filter combination 485DF22 excitation/590DF35 emission. Baseline values ($F_{baseline}$) reflecting the resting potential were measured before the addition of the tool compounds and/or Ca^{2+}/P_i. After the repetitive measurements (F_X), FCCP at a final concentration of 1 μM was added, and fluorescence was measured again (yielding F_{FCCP}). Data were expressed as means of $(F_{FCCP} - F_X)/(F_{FCCP} - F_{baseline})$ for each well ± S.E.M.

For the calibration of the dependence of safranin fluorescence on $\Delta\Psi$, K^+ diffusion potentials were induced by 20 nM valinomycin in the presence of 1 μM rotenone and 2.5 μM oligomycin, as described for JC-1 (5,5′,6,6′-tetrachloro-1,1′,3′-tetraethylbenzimidazolyl-carbocyanine iodide; Reers et al., 1991). K^+ concentrations in the medium were varied from 0.1 to 20 mM, the matrix K^+ ($[K^+]_{in}$) concentration was taken as 120 mM (Rossi and Azzone, 1969), and $\Delta\Psi$ in mV was calculated using the Nernst equation: $\Delta\Psi = -60 \log([K^+]_{in}/[K^+]_{out})$.

Isolation and Culture of Hepatocytes. Hepatocytes were isolated from overnight-fasted male Sprague-Dawley rats (200–250 g) by collagenase perfusion of livers, as described previously (Gores et

al., 1988). Cell viability routinely exceeded 90%, as determined by trypan blue exclusion. Hepatocytes were then cultured in Waymouth's MB-7521/1 medium containing 27 mM $NaHCO_3$, 2 mM L-glutamine, 10% fetal calf serum, 100 nM insulin, and 100 nM dexamethasone. For cell viability assay, hepatocytes were plated onto 24-well microtiter plates (Falcon, Lincoln Park, NJ) coated with 0.1% Type 1 rat-tail collagen at a density of 1.5×10^5 cells/well in 1 ml of medium. For confocal microscopy, hepatocytes were cultured on collagen-coated 40-mm glass coverslips placed in 60-mm plastic Petri dishes at a density of 1 to 2×10^6 hepatocytes/dish in 4 ml of medium. Hepatocytes were used after overnight (14–16 h) incubation in humidified 5% CO_2/95% air at 37°C.

Cell Viability Assay. Viability of hepatocytes cultured on multiwell plates was monitored by propidium iodide fluorometry using a fluorescence scanner (FLUOstar 403; BMG LabTechnologies, Durham, NC). Briefly, hepatocytes in 24-well plates were incubated with 30 μM propidium iodide. Fluorescence from each well was measured using excitation and emission wavelengths of 544 nm (25-nm band pass) and 590 nm (35-mm band pass), respectively. For each experiment, an initial fluorescence measurement (A) was made 20 min after addition of propidium iodide and then at intervals thereafter. Individual experiments were terminated with 375 μM digitonin to permeabilize all cells, and a final fluorescence measurement (B) was obtained 20 min later. The percentage of viable cells (V) was calculated as $V = 100(B - X)(B - A)$, where X is fluorescence at any given time. Cell killing in this assay corresponds to that assessed by trypan blue nuclear staining (Nieminen et al., 1992).

Induction of Apoptosis. Rat hepatocytes were infected with an adenovirus (Ad5IκB) expressing an IκB super-repressor that blocks the antiapoptotic NFκB signaling pathway to sensitize hepatocytes to TNFα-induced apoptosis, as described previously (Bradham et al., 1998), and 2 μM *t*-butylhydroperoxide was added to accelerate the response to TNFα. Briefly, 2 h after plating of hepatocytes, the culture medium was changed to hormonally defined medium (HDM) containing 30 plaque-forming units/cell of Ad5IκB for 2 h at 37°C. After culturing overnight, 2 μM *t*-butylhydroperoxide was added, followed by 30 ng/ml TNFα 1 h later. After 16 h of exposure to TNFα, cell viability was determined by propidium iodide fluorometry.

Confocal Microscopy. For confocal microscopy, TNFα-treated hepatocytes were incubated in HDM supplemented with 25 mM HEPES, pH 7.4, to stabilize pH during confocal measurements. Approximately 30 min before imaging, the hepatocytes were loaded with 250 nM tetramethylrhodamine methyl ester (TMRM) and 1 μM calcein-AM in TNFα-free HDM for 15 min. After loading, the hepatocytes were washed, and the original TNFα-containing HDM was added back. The coverslips were then mounted on the stage of a Zeiss LSM-410 inverted laser scanning confocal microscope in a Focht Chamber System (Bioptechs, Butler, PA) to maintain temperature at 37°C. The green fluorescence of calcein and the red fluorescence of TMRM were excited simultaneously with the 488- and 568-nm lines of an argon-krypton laser. Fluorescence was divided by a 568-nm emission dichroic reflector and recorded by separate photomultipliers through 515 to 565 nm band pass and 590-nm long pass barrier filters. The argon laser was operated at approximately 50% of full power, and the laser output was attenuated with 0.3 to 1% neutral density filters to minimize photodamage and photobleaching. Pinholes were set to 0.9 airy units in the red and green channels to maximize *z*-axis resolution, which was less than 1 μm.

Results

Comparison of Effects of Ca^{2+}/P_i on Swelling and $\Delta\Psi$. The effects of graded concentrations of Ca^{2+} in combination with 1 mM P_i on swelling in the absence or presence of 15 μM safranin and on $\Delta\Psi$ as evidenced by changes in fluorescence at 485/590 nm are shown in Fig. 1A-C. The results show a good temporal correspondence between loss of absorbance and increase in safranin fluorescence as reflected by the decrease of the quotient $(F_{FCCP} - F_X)/(F_{FCCP} - F_{baseline})$ (compare Fig. 1, A and C). Note that the decrease of this quotient occurred more abruptly than the loss of absorbance. This was a consistent finding (see Figs. 3 and 5).

In the absence of safranin, Ca^{2+} concentrations below 50 μM did not induce noticeable swelling. Above 50 μM, increasing Ca^{2+} concentrations caused swelling with progressively decreasing latency. A comparison of Fig. 1, A and B, suggests that the presence of safranin (which caused an upward shift of absorbance by about 0.2 units) slightly promoted the swelling response. In the presence of safranin, the latency to onset of swelling after 50, 75, 100, and 150 μM Ca^{2+} were slightly decreased, and swelling after 30 μM Ca^{2+} began to occur after about 20 min. Corresponding experiments with 10, 20, and 50 μM safranin showed a progressive increase of this promoting effect, but little difference was observed between 10 and 15 μM safranin (data not shown). Because the signal-to-baseline fluorescence ratio was greater with 15 μM safra-

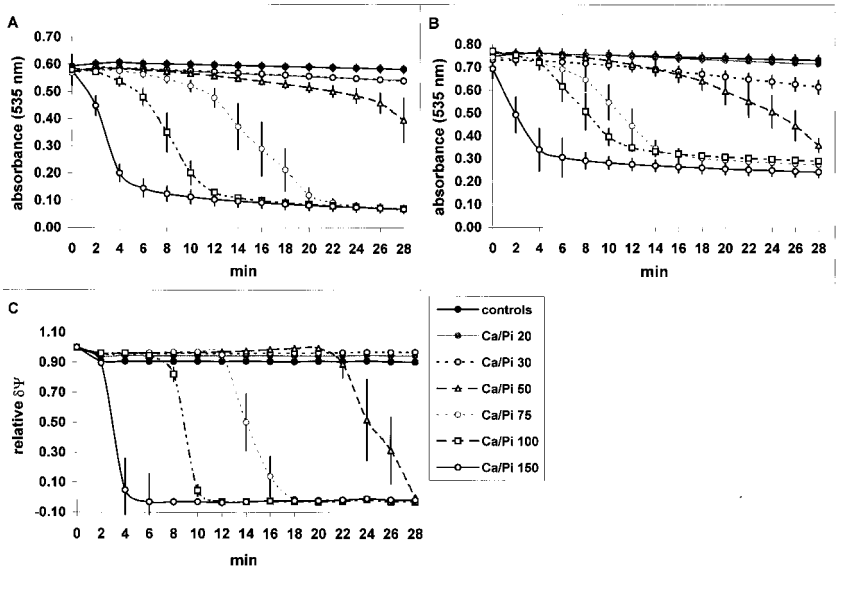

Fig. 1. Effects of graded Ca^{2+} concentrations on swelling in the absence (A) or presence (B) of safranin, and on safranin fluorescence (C) Swelling: 20 μl of mitochondrial preparation and 160 μl RB were added to each well and the baseline values (0 min in the graphs) were measured. Then, 10 μl of Ca^{2+} (graded concentrations) were added with a 12-tip pipette at 10-s intervals per row, followed by 10 μl of P_i 2 min later, also at 10-s intervals per row. Repeated absorbance measurements were started exactly 2 min after addition of Ca^{2+} to the first row. Data are means ± S.E.M. of quadruplicates. Safranin fluorescence: 20 μl of mitochondrial preparation, 150 μl of RB, and 10 μl of safranin (final concentration, 15 μM) were added to each well and the baseline fluorescence ($F_{baseline}$) was measured. The values depend on the concentrations of mitochondrial proteins and range between about 50,000 and 70,000 fluorescence units among different experiments. Ca^{2+}/P_i were added and repetitive fluorescence measurement started as above, yielding F_x values. Fluorescence values obtained after full depolarization ranged between 170,000 and 230,000 among different experiments. After termination of the repetitive measurements, 10 μl of FCCP was added and the plate remeasured once, yielding F_{FCCP}. Data represent $(F_{FCCP} - F_X)/(F_{FCCP} - F_{baseline})$ for each well ± S.E.M. of quadruplicates.

nin, we chose this concentration for the subsequent experiments.

Calibration of ΔΨ Dependence of Safranin Fluorescence. Experiments were run in parallel with 10, 15, and 20 μM safranin in RB, isolation buffer, or the buffer used by Reers et al. (1991) (200 mM sucrose, 20 mM mannitol, 20 mM 4-morpholinopropanesulfonic acid, 1 mM EDTA). The results were very similar; therefore, only those obtained with 15 μM safranin in RB are shown in Fig. 2. A sigmoid relationship between the change in safranin fluorescence and ΔΨ was observed with a practically linear section between −60 and −160 mV. These results showed that safranin fluorescence measurements faithfully reflected changes in ΔΨ in a relevant potential range.

Effects of Cyclosporin Derivatives on Swelling and ΔΨ Changes Caused by Ca^{2+}/P_i. The effects of graded concentrations of CsA, PKF220-384 and NIM 811 on Ca^{2+}/P_i-induced swelling and loss of ΔΨ were compared. Figure 3 shows that all these compounds caused a dose-dependent inhibition of swelling and loss of ΔΨ with partial inhibition beginning at about 0.2 μM. Full inhibition by CsA and NIM811 occurred at 1 μM and greater. PKF220-384 was a little more potent than CsA and NIM811, causing full protection against the MPT at 0.5 μM.

It should be noted here that these potencies were not absolute. With another batch of mitochondria and a smaller Ca^{2+} concentration that takes longer to induce swelling and ΔΨ loss, full protection against the MPT was sometimes obtained with 0.5 μM CsA. The relative potency of CsA, PKF220-384, and NIM811, however, was retained. Partial protection was manifested in a delayed swelling and loss of ΔΨ, resembling the type of curves seen with graded Ca^{2+} concentrations (Fig. 1) and never by reaching a plateau at an intermediate absorbance or ΔΨ. Because the three cyclosporin derivatives were always found to afford full protection from Ca^{2+}/P_i-induced swelling/ΔΨ loss at 1 μM, this concentration was used in further experiments (see below).

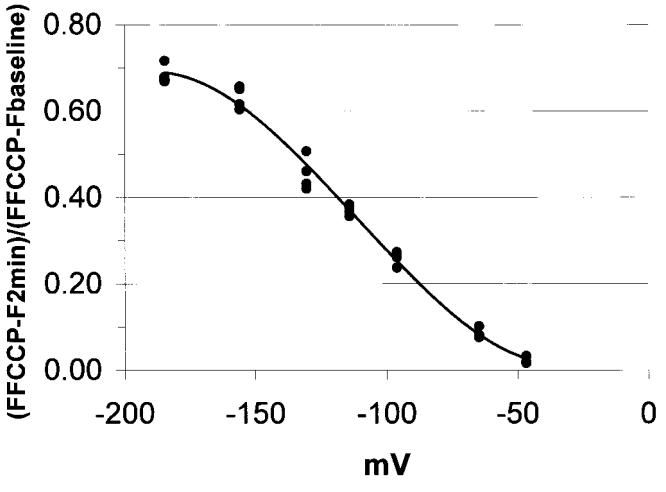

Fig. 2. Calibration of dependence of safranin fluorescence on ΔΨ. To each well of a 96-well plate, 20 μl of mitochondrial preparation containing 200 to 400 μg of mitochondrial protein, 140 μl of RB, 20 μl of RB containing 20 μM rotenone, 200 nM valinomycin, and 50 μM oligomycin (yielding final concentrations of 1 μM rotenone, 20 nM valinomycin and 2.5 μM oligomycin) and 10 μl of RB containing 300 μM safranin (final concentration, 15 μM) were added and the plate read at 485/590 nm, yielding $F_{baseline}$. Then, 10 μl of RB containing graded concentrations of KCl (to reach final concentrations of 0.1, 0.3, 0.8, 1.5, 3, 10, and 20 mM K^+, four wells for each K^+ concentration) were added at intervals of 10 s to each row from top to bottom using a 12-tip pipette. The plate was put into the reader and measurements started such that the first well was read 2 min after pipetting KCl to the first row, yielding F_{2min}. Thereafter, 10 μl of RB containing 20 μM FCCP (final concentration 1 μM) were added and the plate remeasured, yielding F_{FCCP}. From these data, $(F_{FCCP} - F_{2min})/(F_{FCCP} - F_{baseline})$ was calculated for each well and plotted against ΔΨ, calculated using the Nernst equation.

The formyl peptide receptor antagonist CsH did not affect Ca^{2+}/P_i-induced swelling nor the corresponding loss of ΔΨ. The P-glycoprotein inhibitor PSC833 exhibited some protective effect against Ca^{2+}/P_i-induced swelling/ΔΨ loss at 10 μM and a more marked, although incomplete, effect at 30 μM (Fig. 3G/H), which suggests that PSC833 does interact with cyclophilin D to some extent with a potency 10- to 30-fold lower potency than CsA.

Interaction of Cyclosporins with the Effects of Rotenone and MPP^+. Rotenone at 0.1 μM did not induce swelling or affect ΔΨ when added to the mitochondria in the absence of Ca^{2+}/P_i. However, in the presence of Ca^{2+}/P_i, rotenone delayed swelling by about 6 min without affecting the decrease in ΔΨ caused by the Ca^{2+}/P_i (not shown). At 1 μM, rotenone added alone caused a slow, gradual loss of ΔΨ (Fig. 4B) but did not cause swelling (Fig. 4A). In combination with Ca^{2+}/P_i, an immediate and complete collapse of ΔΨ occurred, but the swelling induced by Ca^{2+}/P_i was almost completely prevented. When CsA, PKF220-384, or NIM811 was combined with rotenone plus Ca^{2+}/P_i, no swelling was observed; collapse of ΔΨ was initially as complete as after rotenone plus Ca^{2+}/P_i alone. However, ΔΨ partially recovered thereafter to a maximum extent after about 12 min and then slowly subsided again (Fig. 4, A and B). With 10 μM rotenone, the results were similar except that the rebound of ΔΨ did not occur (not shown).

MPP^+ at 600 μM in the absence of Ca^{2+}/P_i caused a slow and gradual dissipation of ΔΨ without causing swelling in a fashion similar to rotenone (data not shown). In contrast to rotenone, however, MPP^+ enhanced the swelling caused by Ca^{2+}/P_i, as reported previously by Cassarino et al. (1999). MPP^+ also enhanced the Ca^{2+}/P_i-induced loss of ΔΨ, although not as dramatically as rotenone (Fig. 4, C and D). In the presence of CsA, PKF220-384, or NIM811, swelling caused by MPP^+ plus Ca^{2+}/P_i was abolished, but ΔΨ showed the same gradual decrease as that caused by 600 μM MPP^+ alone.

Protection against TNFα-Induced Apoptosis by NIM811. Many cells, including cultured rat hepatocytes, resist TNFα-mediated apoptosis via activation of an NFκB survival pathway (Wang et al., 1996; Bradham et al., 1998). To make hepatocytes sensitive to TNFα, we infected with an IκB (S34A/S36A)-superrepressor expressing adenovirus (Ad5IκB) that prevents activation of antiapoptotic NFκB signaling after TNFα addition (Iimuro et al., 1998). We also exposed the Ad5IκB-infected hepatocytes to a small nontoxic concentration of *t*-butylhydroperoxide (*t*-BuOOH, 2 μM), because preliminary experiments determined that pretreatment in this way accelerated onset of apoptosis after subsequent TNFα addition (T. Qian and J. J. Lemasters, unpublished observations). Ad5IκB and *t*-butylhydroperoxide alone or in combination at the concentrations used did not cause cell killing in the absence of TNFα.

When primary rat hepatocytes treated with Ad5IκB and *t*-BuOOH were exposed to 35 ng/ml TNFα, viability was progressively lost beginning after about 4 h of treatment.

After 16 h, about 70% of cells lost viability (Fig. 5). Cell killing was apoptotic as confirmed by chromatin condensation, nuclear fragmentation, and annexin staining (data not shown). NIM811 in the range of 0.5 to 5 μM caused a dose-dependent inhibition of apoptosis. CsA also caused dose-dependent protection against apoptosis between 0.5 and 2 μM. At higher concentrations of CsA, cell killing increased. By contrast, NIM811 did not cause increased cell killing at high concentrations (Fig. 5).

To monitor directly changes of mitochondrial inner membrane permeability and polarization during the progression of apoptosis, cultured hepatocytes treated with Ad5IκB and *t*-BuOOH were loaded with TMRM and calcein and then exposed to TNFα. Before addition of TNFα, confocal microscopy of the hepatocytes revealed punctate mitochondrial TMRM fluorescence indicative of mitochondrial polarization, whereas calcein fluorescence was confined to the cytosol and outlined individual mitochondria as dark round voids (Fig. 6). Subsequently, beginning slightly after 4 h and essentially complete after 6 h, mitochondria lost their TMRM fluores-

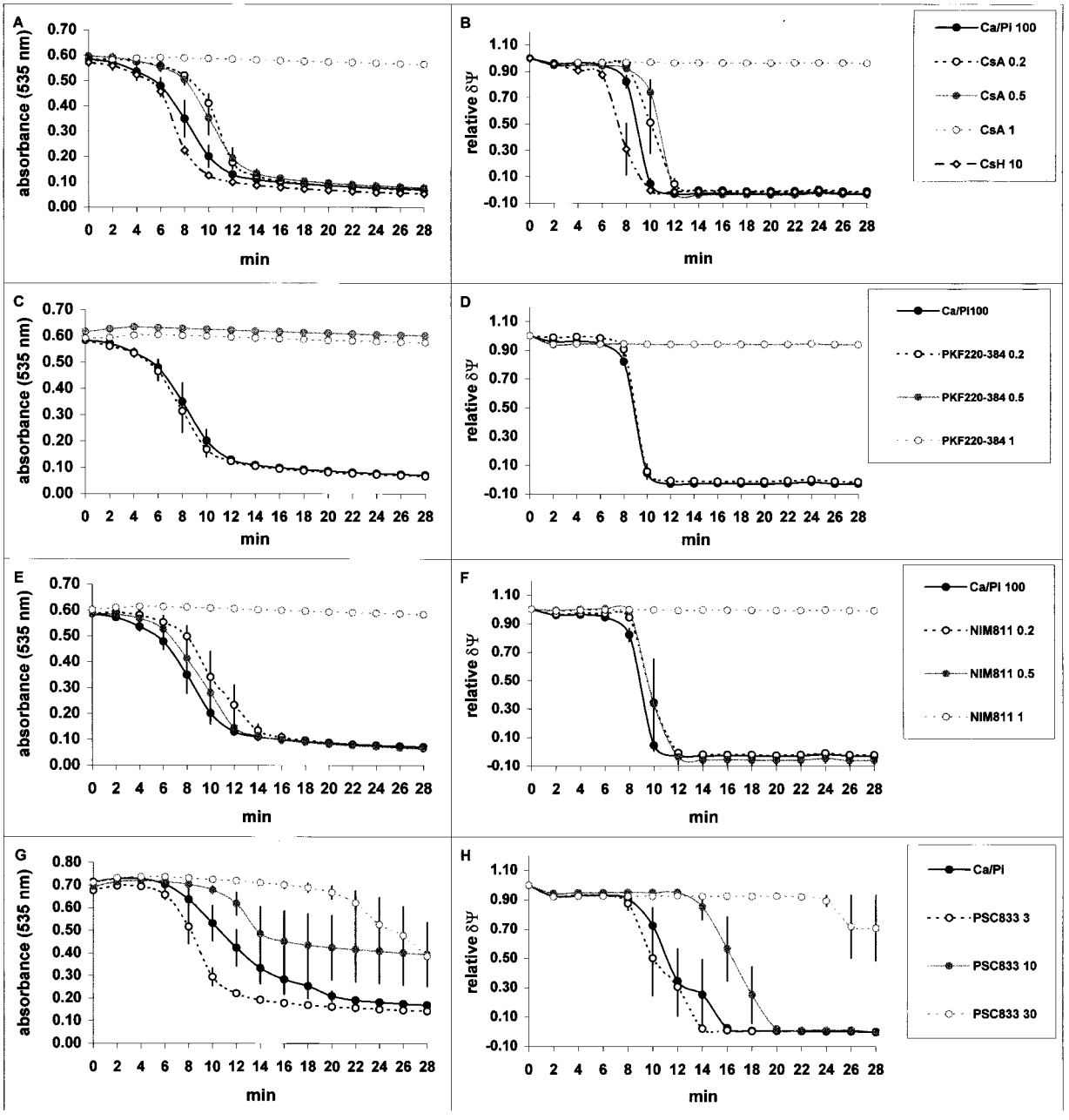

Fig. 3. Prevention of Ca^{2+}/P_i-induced swelling and $\Delta\Psi$ changes by cyclosporin derivatives. The procedure was exactly as described in the legend of Fig. 1. To 20 μl of mitochondrial preparation, 140 μl of RB and 20 μl of RB containing appropriate concentrations of CsA (A and B), CsH (A and B), PKF220-384 (C and D), and NIM811 (E and F) (figures in captions, in micromolar) were added, baseline absorbance was measured, Ca^{2+} (final concentration, 100 μM) and P_i (final concentration, 1 mM) were added, and repetitive absorbance readings were started. For measurements of safranin fluorescence, 130 instead of 140 μl of RB and 10 μl of safranin (final concentration, 15 μM) were added, $F_{baseline}$ was read, Ca^{2+} and P_i were added, F_X read was repetitively, FCCP in 10 μl of RB (final concentration 1 μM) was added and reread. Data are absorbance readings (A, C, E, and G) and $(F_{FCCP} - F_X)/(F_{FCCP} - F_{baseline})$ (B, D, F, and H) ± S.E.M. of quadruplicates. PSC833 (G and H) was measured in a separate experiment, in which a Ca^{2+} concentration of 200 μM was used; everything else was identical.

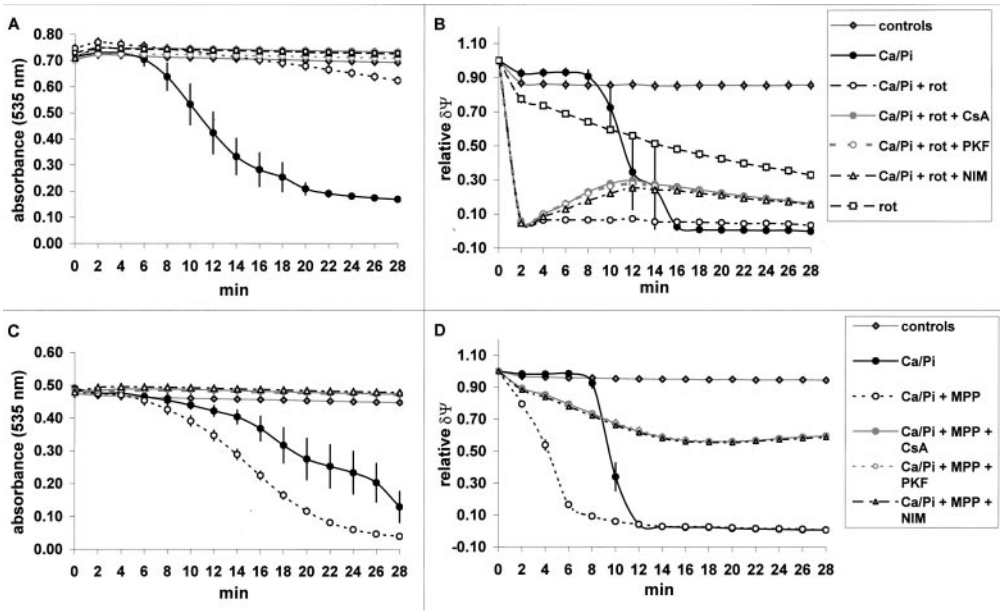

Fig. 4. Combination with rotenone (A and B) and MPP^+ (C and D). To 20 μl of mitochondrial preparation, 130 μl of RB and 20 μl of RB containing 10 μM CsA, PKF220-384, or NIM811 (to reach final concentrations of 1 μM) were added, baseline absorbance was measured, MPP^+ (final concentration, 600 μM) or rotenone (rot; final concentration 1 μM) in 10 μl of RB was added at 10-s intervals per row, followed likewise 2 min later by Ca^{2+} (final concentrations, 50 μM in the MPP^+ experiment and 200 μM in the rotenone experiment) and again 2 min later by P_i (final concentration, 1 mM), and repetitive absorbance readings started. For measurements of safranin fluorescence, 120 instead of 130 μl of RB and 10 μl of safranin (final concentration, 15 μM) were added, $F_{baseline}$ was read, Ca^{2+} and P_i was added, FX was read repetitively, and FCCP in 10 μl of RB (final concentration, 1 μM) was added and reread. Data are absorbance readings (A and C)) and $(F_{FCCP} - F_{2min})/(F_{FCCP} - F_{baseline})$ values (B and D) ± S.E.M. of quadruplicates.

cence and simultaneously filled with calcein. Previous studies showed that this depolarization (loss of TMRM fluorescence) and inner membrane permeabilization (entry of calcein into the matrix space) was blocked by CsA (Bradham et al., 1998).

To characterize the effects of NIM811 on mitochondrial depolarization and inner membrane permeabilization, we exposed hepatocytes to TNFα in the presence of 2 μM NIM811. With NIM811, mitochondrial depolarization and inner membrane permeabilization were prevented and did not occur even after 12 h exposure (Fig. 7). Thus, NIM 811 prevented both onset of the MPT and apoptosis after exposing sensitized hepatocytes to TNFα.

Discussion

Comparative studies of drug effects on the MPT by means of absorbance measurements using the conventional cuvette technique are cumbersome, because the mitochondria have to be freshly prepared by differential centrifugation. By the time they are ready, almost half a day is spent. Moreover, they can be used only for a few hours, because their susceptibility toward induction of the MPT increases with the time elapsed since their preparation (see below). This limits the number of samples that can be evaluated per experiment. Therefore, it was useful to set up an assay that allowed simultaneous measurement of several samples. The most straightforward way to achieve this goal was the microtiterplate format. We developed microtiterplate assays of mitochondrial swelling and $\Delta\Psi$ and used them in the present study to compare the effects of CsA with those of its nonimmunosuppressive derivatives PKF220-384 and NIM811. Swelling was assessed by absorbance decreases, and mitochondrial $\Delta\Psi$ by the fluorescence of safranin, a cationic fluorophore that accumulates into polarized mitochondria in proportion to $\Delta\Psi$ (Akerman and Wikstrom, 1976). Uptake of safranin leads to fluorescence quenching that can be measured with the fluorescence reader (Fiskum et al., 2000).

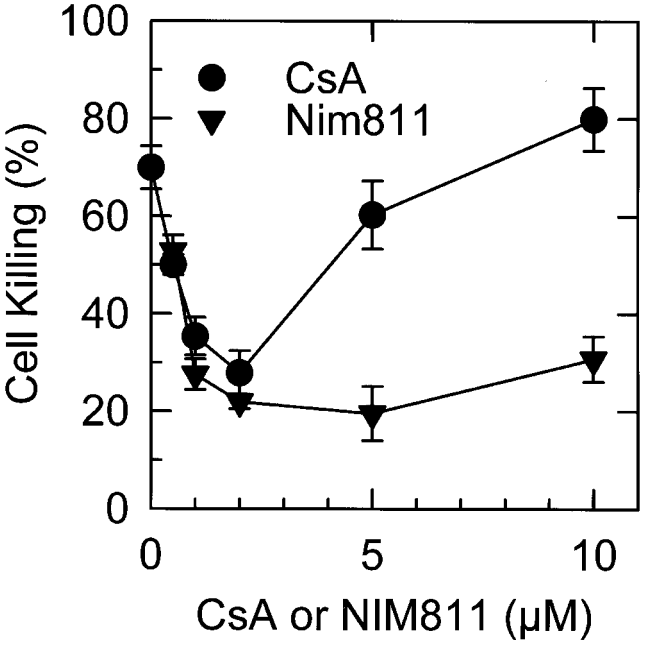

Fig. 5. Inhibition by CsA and Nim811 of TNFα-induced apoptosis in primary cultured rat hepatocytes. Hepatocytes infected with Ad5IkB were treated with *t*-butylhydroperoxide and TNFα, as described under *Experimental Procedures*, in the presence of 0 to 10 μM CsA or Nim811. Cell killing was assessed after 16 h by propidium iodide fluorometry.

To obtain a baseline absorbance providing a suitable absorbance difference in the microtiterplate reader upon MPT

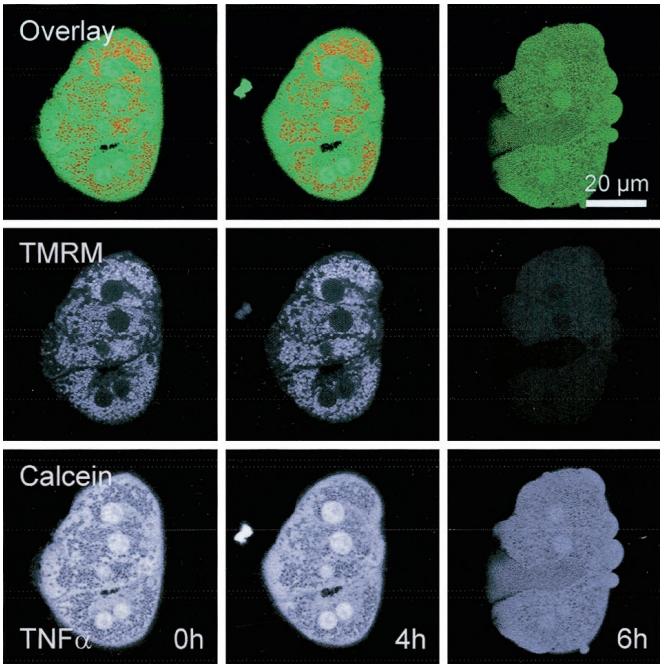

Fig. 6. TNFα-induced onset of the MPT in cultured hepatocytes. Sensitized hepatocytes were loaded with 200 nM TMRM (a potential-indicating fluorophore) and 1 μM calcein AM (a probe of membrane permeability) and exposed to TNFα, as described under *Experimental Procedures* and Fig. 5. The red fluorescence of TMRM and green fluorescence of calcein were imaged by confocal microscopy. Note that after 6 h of exposure to TNFα, mitochondria depolarized and the inner membrane became permeable, as indicated by release of TMRM fluorescence from individual mitochondria and redistribution of calcein from the cytosol into mitochondria.

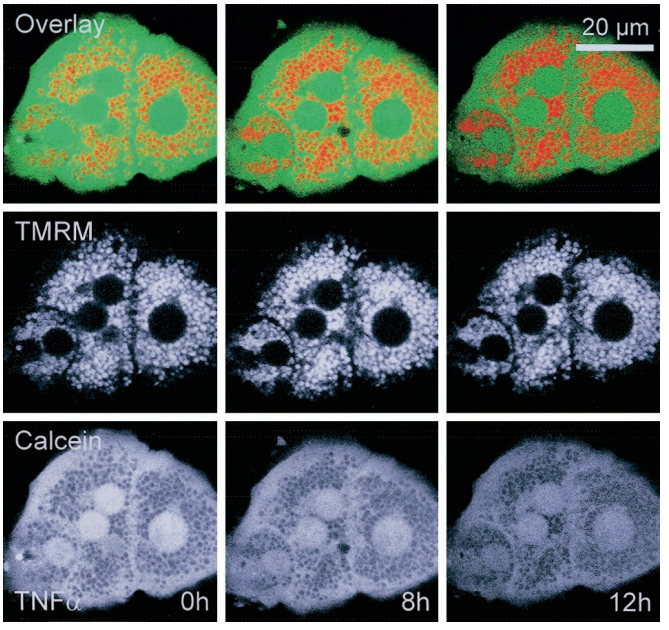

Fig. 7. Inhibition by NIM811 of TNFα-induced onset of the MPT in cultured hepatocytes. Sensitized hepatocytes were treated with TNFα in the presence of 2 μM Nim811 and loaded with TMRM and calcein, as described in Fig. 6. In the presence of Nim811, the MPT was blocked, as indicated by no loss of red mitochondrial TMRM fluorescence and the absence of redistribution of calcein fluorescence into mitochondria.

induction, a concentration of 1 to 2 mg/ml mitochondrial protein in the wells was necessary. Although a lower concentration of mitochondrial protein would have sufficed for the $\Delta\Psi$ measurements with safranin, it seemed essential for comparability between absorbance and $\Delta\Psi$ to maintain this mitochondrial concentration and all other parameters constant. Accordingly, a relatively high safranin concentration was needed to provide good fluorescence signals. The calibration of the safranin response using K^+ diffusion potentials (Fig. 2) indicated that safranin fluorescence was sensitive to $\Delta\Psi$ changes over the potential range of interest for the conditions used.

The susceptibility of rat liver mitochondria to MPT induction by Ca^{2+} measured by absorbance can vary from one preparation to another. The minimal Ca^{2+} concentration causing maximal absorbance loss within 12 min after exposure ranged between 75 and 300 μM in over 50 experiments but was 100 or 150 μM in about 70% of the cases. Moreover, this susceptibility increased with the time elapsed after mitochondrial isolation. On average, the MPT occurred twice as fast after 3.5 h compared with 30 min after finishing the preparation of mitochondria. Although variation from one preparation to another occurred, the increase of susceptibility with time after isolation always occurred. This should be borne in mind when the presented absorbance and $\Delta\Psi$ data are compared, because they were not obtained simultaneously, but sequentially. Although matching 'absorbance' and 'safranin' plates were always read immediately one after the other in this sequence, a time difference of 30 to 40 min could not be avoided. Therefore, a small lead of the $\Delta\Psi$ changes over the corresponding absorbance decreases should not be interpreted as significant. For these reasons, we conclude from the obtained data that changes in absorbance and $\Delta\Psi$ after exposure of mitochondria to Ca^{2+}/P_i occurred virtually simultaneously within the temporal resolution of our experimental setup. This correspondence was maintained if the effects of Ca^{2+}/P_i were enhanced by the prooxidant, *t*-BuOOH.

MPP^+ at 600 μM enhanced the absorbance loss caused by Ca^{2+}/P_i and similarly enhanced the Ca^{2+}/π-induced dissipation of $\Delta\Psi$, in agreement with the report of Cassarino et al. (1999) who ascribed this to an increase in the production of oxygen radicals. Rotenone, in contrast, delayed and at higher concentrations prevented Ca^{2+}/π-induced swelling, also as described by Cassarino et al. (1999). This inhibition by rotenone is probably caused by its inhibition of NADH-linked respiration (Chernyak and Bernardi, 1996). More efficient than 600 μM MPP^+, rotenone rapidly and completely dissipated $\Delta\Psi$ in the presence of Ca^{2+}/P_i. Alone, rotenone, like MPP^+, caused a slow, gradual loss of $\Delta\Psi$. It seems plausible to attribute these effects of rotenone and MPP^+ on $\Delta\Psi$ to complex I inhibition. The difference between MPP^+ and rotenone on changes to $\Delta\Psi$ supports the idea that the neurotoxicity and effect on the MPT of MPP^+ are not simply caused by complex I inhibition (Cassarino et al., 1999; Nakamura et al., 2000).

Ca^{2+}/π-induced swelling and $\Delta\Psi$ dissipation were prevented by CsA, NIM811 and PKF220-384. PKF220-384 was about twice as potent as CsA and NIM811. The concentration-response relationships were very steep. The formyl peptide receptor antagonist CsH (de Paulis et al., 1996) was ineffective on both swelling and loss of $\Delta\Psi$ at 10 μM, but the P-glycoprotein inhibitor PSC833 did block the MPT at 30 μM, in agreement with its weak interaction with cyclophilin D (Perkins et al., 1998). In additional experiments not shown here, CsA, NIM811, and PKF220-384 at 1 μM also com-

pletely prevented swelling and $\Delta\Psi$ dissipation induced by the combination of Ca^{2+}/P_i with the enhancing agents atractyloside, PK11195, and the prooxidant *t*-butylhydroperoxide. Ca^{2+}/π-induced swelling enhanced by 0.1 μM FCCP (which by itself is ineffective despite lowering $\Delta\Psi$) was also completely abolished by CsA, NIM811, and PKF220-384 without alteration of the effect of the uncoupler on $\Delta\Psi$. Although the cyclosporins abolished the induction of swelling by the combination of MPP^+ and Ca^{2+}/P_i, the loss of $\Delta\Psi$ was attenuated but not entirely prevented. The pattern obtained with rotenone was different in that the cyclosporins did not affect the initial collapse of $\Delta\Psi$ by rotenone + Ca^{2+}/P_i but did promote a subsequent partial repolarization.

NIM811 also inhibited apoptosis in Ad5IκB-sensitized hepatocytes exposed to TNFα. Cytoprotection by NIM811 was associated with prevention of the MPT, as indicated by the blockade of mitochondrial depolarization and inner membrane permeabilization that otherwise occurred after TNFα treatment. Prevention by NIM of apoptosis and the MPT in cultured hepatocytes was the same as that observed previously by CsA (Bradham et al., 1998). These findings support the conclusion that a CsA- and NIM811-sensitive MPT occurs during apoptotic signaling in TNFα-treated hepatocytes. This MPT causes mitochondrial depolarization and inner membrane depolarization and leads to mitochondrial swelling and release of proapoptotic intermembrane proteins, such as cytochrome *c*.

The cytoprotective effects of CsA and NIM811 were identical only at lower concentrations (0.5–2 μM). At higher concentrations (5–10 μM), CsA lost efficacy. Such a biphasic dose-response curve for CsA has been described previously in experiments with isolated myocytes, perfused hearts, and hepatocytes (Nazareth et al., 1991; Griffiths and Halestrap, 1993; Qian et al., 1997). At high concentrations, cyclosporin A is cytotoxic (Ruiz-Cabello et al., 1994; Jiang and Acosta, 1995). This toxicity may overcome the beneficial effect of CsA on the MPT. By contrast, the efficacy of NIM811 was not lost at higher concentrations. The differential efficacy of NIM811 and CsA may be related to the different effects of these cyclosporin derivatives on calcineurin. Thus, loss of protection by CsA at high concentration may be cytotoxicity caused by inhibition of calcineurin. For this reason, NIM811 seems to be more efficacious than CsA in preventing injury in intact cells.

In conclusion, the present results suggest that the nonimmunosuppressive cyclosporin derivative, NIM811, affects the MPT in much the same way as CsA and PKF220-384, another nonimmunosuppressive derivative. The latter was used in the past to discriminate between MPT- and calcineurin-related effects of CsA in studies of cell protection but is no longer available. NIM811 may fill this gap.

References

Akerman KE and Wikstrom MK (1976) Safranine as a probe of the mitochondrial membrane potential. *FEBS Lett* **68:**191–197.

Bradham CA, Qian T, Streetz K, Trautwein C, Brenner DA, and Lemasters JJ (1998) The mitochondrial permeability transition is required for TNFα-mediated apoptosis and cytochrome *c* release. *Mol Cell Biol* **18:**6353–6364.

Cassarino DS, Parks JK, Parker WD Jr, and Bennett JP Jr (1999) The parkinsonian neurotoxin MPP^+ opens the mitochondrial permeability transition pore and releases cytochrome *c* in isolated mitochondria via an oxidative mechanism. *Biochim Biophys Acta Mol Basis Dis* **1453:**49–62.

Chernyak BV and Bernardi P (1996) The mitochondrial permeability transition pore is modulated by oxidative agents through both pyridine nucleotides and glutathione at two separate sites. *Eur J Biochem* **238:**623–630.

de Paulis A, Ciccarelli A, de Crescenzo G, Cirillo R, Patella V, and Marone G (1996) Cyclosporin H is a potent and selective competitive antagonist of human basophil activation by *N*-formyl-methionyl-leucyl-phenylalanine. *J Allergy Clin Immunol* **98:**152–164.

Fiskum G, Kowaltowksi AJ, Andreyev AY, Kushnareva YE, and Starkov AA (2000) Apoptosis-related activities measured with isolated mitochondria and digitonin-permeabilized cells. *Methods Enzymol* **322:**222–234.

Gores GJ, Nieminen A-L, Fleishman KE, Dawson TL, Herman B, and Lemasters JJ (1988) Extracellular acidosis delays onset of cell death in ATP-depleted hepatocytes. *Am J Physiol* **255:**C315–C322.

Griffiths EJ and Halestrap AP (1993) Protection by cyclosporin A of ischemia/reperfusion-induced damage in isolated rat hearts. *J Mol Cell Cardiol* **25:**1461–1469.

Halestrap AP, Connern CP, Griffiths EJ, and Kerr PM (1997) Cyclosporin A binding to mitochondrial cyclophilin inhibits the permeability transition pore and protects hearts from ischaemia/reperfusion injury. *Mol Cell Biochem* **174:**167–172.

He L and Lemasters JJ (2002) Regulated and unregulated mitochondrial permeability transition pores: a new paradigm of pore structure and function. *FEBS Lett* **512:**1–7.

Iimuro Y, Nishiura T, Hellerbrand C, Behrns KE, Schoonhoven R, Grisham JW, and Brenner DA (1998) NFkappaB prevents apoptosis and liver dysfunction during liver regeneration. *J Clin Invest* **101:**802–811.

Jiang T and Acosta D (1995) Mitochondrial Ca^{2+} overload in primary cultures of rat renal cortical epithelial cells by cytotoxic concentrations of cyclosporine: a digitized fluorescence imaging study. *Toxicology* **95:**155–166.

Kroemer G and Reed JC (2000) Mitochondrial control of cell death. *Nature (Lond) Med* **6:**513–519.

Li PA, Kristián T, He QP, and Siesjö BK (2000) Cyclosporin A enhances survival, ameliorates brain damage and prevents secondary mitochondrial dysfunction after a 30-minute period of transient cerebral ischemia. *Exp Neurol* **165:**153–163.

Matsuura K, Kabuto H, Makino H, and Ogawa N (1996) Cyclosporin A attenuates degeneration of dopaminergic neurons induced by 6-hydroxydopamine in the mouse brain. *Brain Res* **733:**101–104.

Nakamura K, Bindokas VP, Marks JD, Wright DA, Frim DM, Miller RJ, and Kang UJ (2000) The selective toxicity of 1-methyl-4-phenylpyridinium to dopaminergic neurons: the role of mitochondrial complex I and reactive oxygen species revisited. *Mol Pharmacol* **58:**271–278.

Nazareth W, Nasser Y, and Crompton M (1991) Inhibition of anoxia-induced injury in heart myocytes by cyclosporin A. *J Mol Cell Cardiol* **23:**1351–1354.

Nieminen A-L, Gores GJ, Bond JM, Imberti R, Herman B, and Lemasters JJ (1992) A novel cytotoxicity assay using a multi-well fluorescence scanner. *Toxicol Appl Pharmacol* **115:**147–155.

Nieminen A-L, Saylor AK, Tesfai SA, Herman B, and Lemasters JJ (1995) Contribution of the mitochondrial permeability transition to lethal injury after exposure of hepatocytes to *t*-butylhydroperoxide. *Biochem J* **307:**99–106.

Perkins ME, Wu TW, and Le Blancq SM (1998) Cyclosporin analogs inhibit in vitro growth of Cryptosporidium parvum. *Antimicrob Agents Chemother* **42:**843–848.

Petronilli V, Nicolli A, Costantini P, Colonna R, and Bernardi P (1994) Regulation of the permeability transition pore, a voltage-dependent mitochondrial channel inhibited by cyclosporin A. *Biochim Biophys Acta* **1187:**255–259.

Qian T, Nieminen A-L, Herman B, and Lemasters JJ (1997) Mitochondrial permeability transition in pH-dependent reperfusion injury to rat hepatocytes. *Am J Physiol* **273:**C1783–C1792.

Reers M, Smith TW, and Chen LB (1991) J-aggregate formation of a carbocyanine as a quantitative fluorescent indicator of membrane potential. *Biochemistry* **30:**4480–4486.

Rosenwirth B, Billich A, Datema R, Donatsch P, Hammerschmid F, Harrison R, Hiestand P, Jaksche H, Mayer P, and Peichl P (1994) Inhibition of human immunodeficiency virus type 1 replication by SDZ NIM 811, a nonimmunosuppressive cyclosporine analog. *Antimicrob Agents Chemother* **38:**1763–1772.

Rossi E and Azzone GF (1969) Ion transport in liver mitochondria. Energy barrier and stoicheometry of aerobic K+ translocation. *Eur J Biochem* **7:**418–426.

Ruiz-Cabello J, Buss WC, Collier SW, Glazer RI, and Cohen JS (1994) Changes in ATP after cyclosporin A treatment in a renal epithelial cell line in the rat studied by ^{31}P-NMR spectroscopy. *Res Commun Mol Pathol Pharmacol* **86:**3–13.

Scheff SW and Sullivan PG (1999) Cyclosporin A significantly ameliorates cortical damage following experimental traumatic brain injury in rodents. *J Neurotrauma* **16:**783–792.

Schnaitman C and Greenawalt JW (1968) Enzymatic properties of the inner and outer membranes of rat liver mitochondria. *J Biol Chem* **38:**158–175.

Seaton TA, Cooper JM, and Schapira AHV (1998) Cyclosporin inhibition of apoptosis induced by mitochondrial complex I toxins. *Brain Res* **809:**12–17.

Trost LC and Lemasters JJ (1997) Role of the mitochondrial permeability transition in salicylate toxicity to cultured rat hepatocytes: implications for the pathogenesis of Reye's syndrome. *Toxicol Appl Pharmacol* **147:**431–441.

Wang CY, Mayo MW, and Baldwin AS Jr (1996) TNF- and cancer therapy-induced apoptosis: potentiation by inhibition of NF-kappaB. *Science (Wash DC)* **274:**784–787.

Zamzami N, Marchetti P, Castedo M, Hirsch T, Susin SA, Masse B, and Kroemer G (1996) Inhibitors of permeability transition interfere with the disruption of the mitochondrial transmembrane potential during apoptosis. *FEBS Lett* **384:**53–57.

Zamzami N, Brenner C, Marzo I, Susin SA, and Kroemer G (1998) Subcellular and submitochondrial mode of action of Bcl-2-like oncoproteins. *Oncogene* **16:**2265–2282.

Zenke G, Baumann G, Wenger R, Hiestand P, Quesniaux V, Andersen E, and Schreier MH (1993) Molecular mechanisms of immunosuppression by cyclosporins. *Ann NY Acad Sci* **685:**330–335.

Zoratti M and Szabò I (1995) The mitochondrial permeability transition. *Biochim Biophys Acta* **1241:**139–176.

Address correspondence to: Dr. Peter C. Waldmeier, Nervous System Research, Novartis Pharma Ltd., WKL-125.607, CH-4002 Basel, Switzerland. E-mail: peter.waldmeier@pharma.novartis.com